ORIGINAL RESEARCH

Submitted: 21.10.2022; Accepted: 18.11.2022; Published online: 25.12.2022

Biosynthesis of zinc oxide nanoparticles using *saccharomyces boulardii* and study their biological activities

Adil Hakeem Mohamed*, S.W. Kadium

Department of Biology, Faculty of Science, University of Kufa, Iraq.

*Corresponding author:
adil.algeze@gmail.com

Abstract

Objective: Saccharomyces boulardii, a probiotic, is used in the current study's manufacture of zinc oxide nanoparticles with the aim of assessing their biological activity. Due to its advantages over the chemical and physical techniques of synthesis in terms of affordability and environmental friendliness, the biological way of creating nanoparticles is becoming increasingly relevant. **Methods:** Zinc acetate was added at a dose necessary to biosynthesize ZnO NPs from S. boulardii's cell-free supernatant (1 mM). **Results:** An evidence that S. bularedii was responsible for the reaction mixture's color change from light to dark after 150 rpm of incubation was the color change and antibacterial behavior. Atomic force microscopy, scanning electron microscopy, energy dispersive spectroscopy, ultraviolet-visible spectroscopy, and X-ray diffraction (XRD) all contributed to the completion of the characterisation (AFM). The spectra of the ZnO NPs produced in the reaction mixture using UV-visible spectroscopy were (343.75 nm). The XRD showed that ZnO NPs' crystal size was (13.31 nm). The SEM was provided; the shape was uniform and spherical, and the average size (24.61 nm). EDS was used to analyze the presence of elemental ZnO NPs. ZnO NPs' three-dimensional structure was seen using AFM, and their average diameter was (62.89 nm). The FTIR spectrum reveals a variety of functional groups that are present at various locations.

Gram positive and gram negative bacteria that were isolated from diabetic foot infections were multidrug resistant (MDR), and biosynthesized ZnO NPs demonstrated antibacterial action against these bacteria. (*Staphylococcus aureus, Escherichia coli, Klebsiella pneumoniae, Pseudomonas aeruginosa and Proteus mirabilis*). All of the studied bacterial isolates showed the ability to produce biofilms in the form of nanoparticle-treated biofilms on microtiter plates. When pathogenic bacteria were treated with ZnO NPs, this ability was stopped and eliminated. The ZnO NPs (1 mg/ml, 0.5 mg/ml, 0.25 mg/ml, and 0.12 mg/ml) demonstrated their antioxidant ability in vitro by scavenging DPPH free radicals. The combination of DPPH and biogenic ZnONPs at concentration 1 mg/ml showed the highest inhibitory titer (73.79%).

Keywords

Biosynthesis ZnO NPs, Saccharomyces boulardii, Antibiofilm, Antimicrobial, Antioxidant Activity.

Imprint

Adil Hakeem Mohamed, S.W. Kadium. Biosynthesis of zinc oxide nanoparticles using saccharomyces boulardii and study their biological activities. Cardiometry; Special issue No. 25; December 2022; p. 41-50; DOI: 10.18137/cardiometry.2022.25.4150; Available from: http://www.cardiometry.net/issues/no25-december-2022/biosynthesis-zinc-oxide

INTRODUCTION

For diabetic patients, diabetic foot infections (DFIs) are a significant clinical and cost burden (Veve et al 2022). One of the most dreaded effects of diabetes are DFIs, which can develop quickly into permanent septic gangrene and need foot amputation. Up to 70% of all limb amputations are performed on diabetics, who also have a 25 times higher risk of losing a leg than persons without the condition (Singh et al 2005). Non-pathogenic yeast Saccharomyces boulardii has been used for a long time as a probiotic agent to prevent or cure a number of gastrointestinal diseases in humans, including antibiotic-associated diarrhea (Dahiya & Nigam, 2022). In order to manufacture nano-sized particles, nanobiotechnology combines biological principles with physical and chemical methods (1-100nm) It offers a practical substitute for expensive chemical and physical ways of producing nanoparticles with precise functionality. Based on fundamental traits including scale, distribution, and shape, nanoparticles can have new or changed features. Applications for NPs and nanomaterials are being developed more often (Begum et al 2022). Because of its numerous uses in biotechnology and bioengineering as antibacterial, antifungal, antioxidant, and tools for preventing the formation of biofilms, zinc oxide nanoparticles (ZnO NPs) have drawn significant interest (Zhang et al 2022). In order to explore the antibacterial, antibio-

film, and antioxidant properties of ZnO NPs utilizing S. boulardii species, the current study was created.

EXPERIMENTAL

Preparation supernatant of *S. boulardii*

Saccharomyces boulardii was carefully selected from a variety of yeast species based on its resistance to industrial ZnO NPs and its capacity to produce ZnO NPs extracellularly (in the supernatant). S. boulardii was injected into Sabouraud dextrose broth (SDB), which was then incubated for 24 hours at 37°C. For 25 minutes at 4°C and 6000 rpm, the culture was centrifuged to separate the S. boulardii supernatant. It was decided to create cell-free supernatants for the production of zinc oxide nanoparticles. **(Mohd Yusof *et al* 2020).**

Biosynthesis of ZnO NPs using cell free supernatant

S. boulardii used zinc acetate as the precursor for the production of ZnO NPs. To the cell-free supernatant, zinc acetate was added at a concentration of 1 mM and stirred. The resulting solutions were incubated for 24 hours at 37° C in a shaking incubator at 150 rpm. After incubation, the reaction mixture was centrifuged at 6000 rpm for 25 min. at 4°C to remove the supernatant. The supernatant was then replaced with deionized distill water, and the centrifugation process was repeated three more times under the same conditions to remove any remaining supernatant. The pellet-shaped collection of nanoparticles was then dried in an oven at 40°C for 18 to 24 hours. The dry powder was carefully gathered and kept in storage for additional investigation. **(Ramesh *et al* 2021).**

Characterization of ZnO nanoparticles

Visible UV ZnO NPs were characterized using X-ray diffraction and spectroscopy. In the electron microscopy unit, SEM was utilized to characterize the morphology of nanoparticles. The microscope functioned with variable magnifications, low vacuum, a spot size of 4, and working distances of 5–10 mm at an accelerated voltage of 15 KV (Shafaghat, 2015). Utilizing Bruker EDS coupled with SEM, elemental analysis of a single particle was performed. EDS was utilized to do a point analysis with an accelerating voltage of 10 KV, a spot size of 5, and working distances of 10 mm (Shirley & Jarochowska 2022). The ZnO NPs were characterized using AFM. The FTIR spectrophotometer was used to measure the synthesized formulations' transmittance.

Antibacterial activity of ZnO nanoparticles

Biogenic ZnO NPs' antibacterial activity was delivered by agar well diffusion against several pathogenic, multi-drug resistant gram positive and gram negative bacteria isolated from diabetic foot infections. Each tested bacterium was suspended to the McFarland standard (0.5N) and then swabbed individually onto sterile Muller-Hinton Agar (MHA) plates. Agar was pierced with a 7 mm sterilized cork borer, and 100 l of biogenic ZnO NPs were added to each well at various concentrations (50, 100, and 200 g/ml), which were then incubated for 24 hours at 37 °C. The inhibitory zones were then quantified. **(Rajeshkumar and Malarkodi, 2014).**

Antibiofilm activity of zinc oxide nanoparticles

As the gold standard test for biofilm formation detection, we employed the Tissue Culture Plate Approach or Microtiter Plate Method. This method allowed us to quantitatively evaluate biofilm development and antibiofilm activity by nanoparticles. (**Barapatre *et al* 2016**).

Antioxidant activity of biogeneic zinc oxide nanoparticles in vitro

The capacity of the extracts to scavenge free radicals was assessed using the DPPH (2,2-diphenyl-1-picrylhydrazyl). In methanol, the DPPH solution (0.006% w/v) was created. 96-well plates are used. 200 L of freshly made DPPH solution was added to the control well, 200 L of methanol was added to the blank well, 100 L of ZnO NPs (1 mg/ml, 0.5 mg/ml, 0.25 mg/ml, 0.12 mg/ml) were added to each well's DPPH solution, and the final volume was 200 L. After 30 minutes of incubation in the dark, discoloration was measured at 517 The control was DPPH solution.

Using the following equation, the percentage of DPPH free radical scavenging was determined:

DPPH scavenging impact (%) = (Ao –A1) / Ao X 100

Where Ao was the absorbance of the control and A1 was the absorbance in the presence of the ZnO NPs **(Goyal *et al* 2010).**

RESULTS AND DISCUSSION

Biosynthesis of zinc oxide nanoparticles

The extracellular production of ZnO NPs by Saccharomyces boulardii was demonstrated utilizing cell free supernatant and zinc acetate (1Mm) as a precursor. The free cell supernatant of S. boulardii is able to alter the color of the reaction mixture after being incubated for 24 hours at 37°C and 150 rpm while being shaken, which serves as an indication for the biosynthesis of ZnO NPs. The microbial cell secretes reductases that are used in the bio reduction of metal ions into the appropriate NPs during the extracellular creation of nanoparticales (Ovais et al., 2018). The antibacterial behavior and the reaction mixture's color change from light to dark after 150 rpm incubation provided as evidence that S. bularedii was responsible for the ZnO NPs' production. In contrast to the cell, where the components in the cytoplasm would strive to maintain a steady environment and call for more purification, the environment of the culture supernatant may be simply improved. Therefore, rather of using cells themselves, supernatant may be utilized to make zinc oxid nanoparticles (Bahrulolum et al., 2021). Numerous investigations have suggested that the creation of metal nanoparticles involves NADH and NADH-dependent enzymes. It appears that the reduction was initiated by the NADH-dependent reductase acting as an electron transporter to transfer electrons from the NADH (Ranganath et al., 2012; Joerger et al., 2000). The morphology depends on a number of chemical and physical factors, including incubation period, pH, the makeup of the culture media, and whether the organism grows in the light or the dark. **(Durán *et al.*, 2011).**

UV-visible Spectroscopy

When ZnO NPs were analyzed using UV-vis spectrophotometry, an absorption peak at 343.75 nm wavelength was seen, showing that ZnO NPs were present in the reaction solution. **figure (1).**

Visual inspection and UV-vis spectroscopy measurements of the surface plasmon resonance (SPR) band can both attest to the biogenesis of nanoparticles. Nanoparticles' single SPR band demonstrates their spherical form. **(Abdulhassan, 2016).**

XRD analysis of nanoparticles

S. boulardii formed ZnO NPs with average crystal sizes of 13.31 nm, according to the XRD, figure (2).

Intense peaks at 2 corresponding to about the lattice plane indices were seen in the X-ray diffraction pattern of ZnO NPs produced extracellularly by S. boulardii, Table (1).

Table (1)

Lattice planes resulted by the ZnO NPs that correspond to the ZnO, Hexagonal standard card (PDF#36-1451).

h k l index	Source of ZnO NPs
	S. boulardii
100	31.409 (2θ)
002	34.055 (2θ)
101	35.916 (2θ)
102	47.218 (2θ)
110	56.271 (2θ)
103	62.578 (2θ)
112	67.66 (2θ)

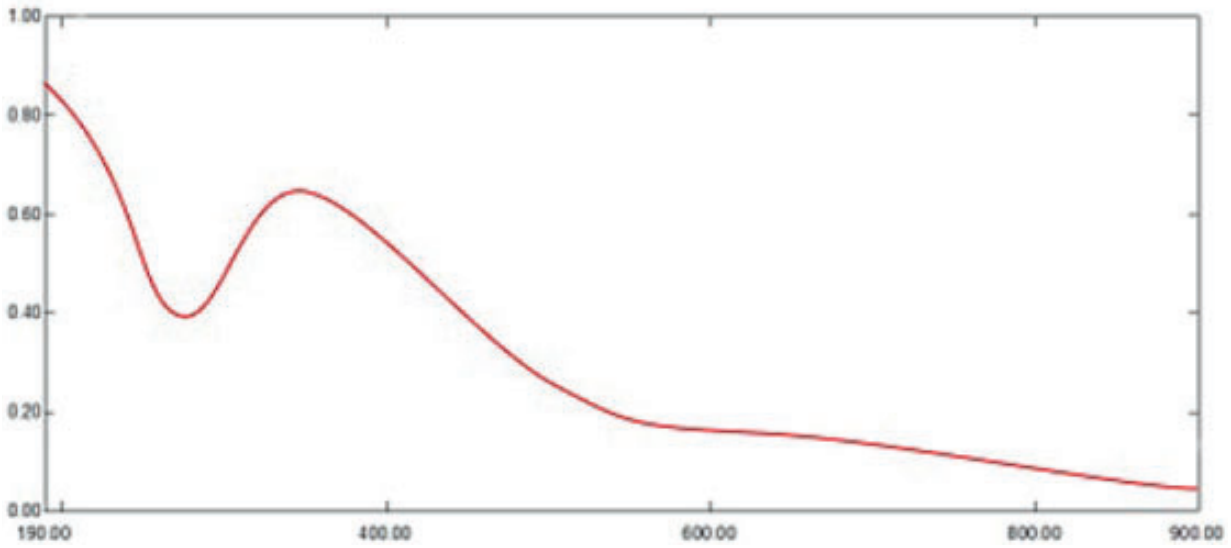

Figure (1): UV-visible spectroscopy analysis of ZnO NPs synthesis by S. bularedii

Their crystalline structure is shown by the peaks' sharpness in the XRD spectrum (Yallappa et al 2013). The ZnO NPs biosynthesized from S. boulardii were 13.31 nm in size, which is different from the typical size ranges shown in (Loganathan, et al., 2021) by 64.74 nm.

SEM analysis of ZnO NPs

The SEM findings revealed well-dispersed nanoparticles and homogeneous ZnO NPs with an average size of 24.61 nm and spherical shape (Figure) (3).

In accordance with the findings of Dobrucka & Dugaszewska, biogenic ZnO NPs were agglomerated

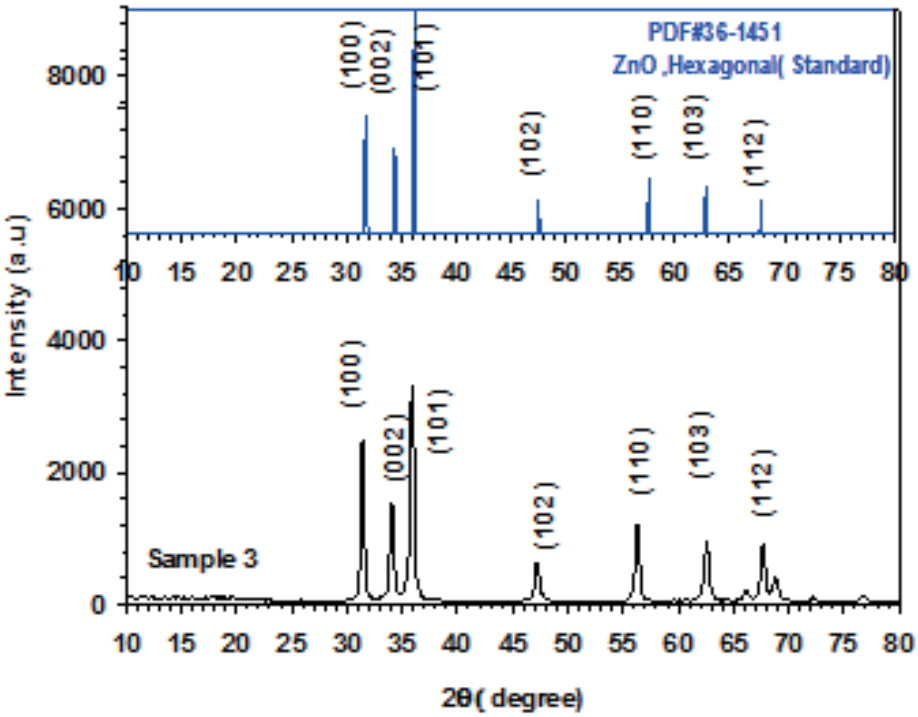

Figure (2) reveals the XRD pattern and quantitative analysis of the sample ZnO NPs as synthesized by *S. boulardii.* The XRD of the NPs formed diffraction peaks that correspond to the ZnO, Hexagonal standard card (PDF#36-1451).

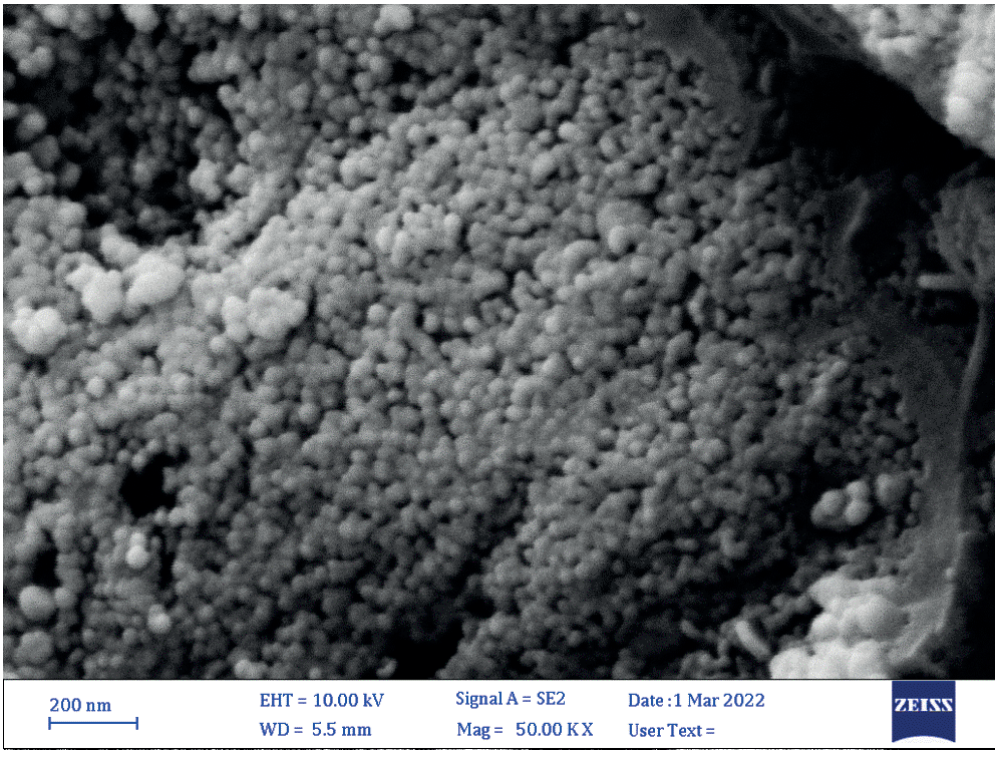

Figure (3): SEM micrograph of biogenic ZnO NPs. The shape of ZnO NPs was spherical and homogenous, Size average (24.61 nm).

with a spherical shape using the SEM to define the shape and size of the nanoparticles.

EDS analysis of nanoparticles

The presence of elemental zinc oxide indicated that S. boulardii supernatant had reduced the zinc ions in the mixture. Strong signals from the Zn atoms, medium signals from oxygen, and weaker signals from other elements were seen in the EDS spectrum that was captured in point and map mode. Zn had an elemental component weight percentage of 82.9% and an oxygen content of 9.8% (Figure (4), Table) (2).

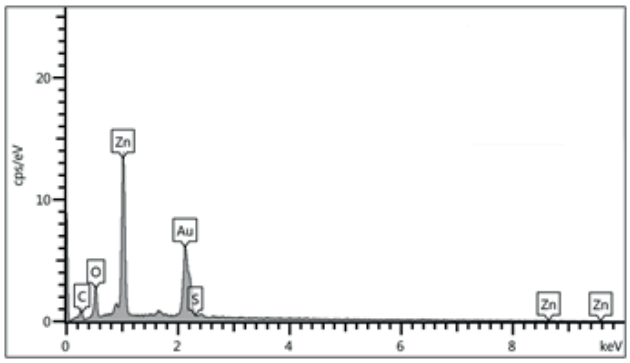

Figure (4): EDS analysis (point and mapping) of biogenic zinc oxide nanoparticles: Illustrated strong signals from the Zn, medium signal from O2, the optical absorption peak of Zn was observed at 3Kev, the weight percentage of zinc (82.9%).

Table (2)

Elemental analysis of ZnO NPs nanocomposite

Elements	Wt %
Zn	82.9
O	9.8
C	6.4
S	0.8

The incident ZnO NPs were measured using (EDS) analysis by looking at the optical absorption peaks of the zinc oxide components. The presence of elemental zinc demonstrated that ions were reduced throughout the microorganism's response. Strong signals from the NPs atoms were seen in the EDS spectra when it was captured in spot-profile mode, compared to medium signals from oxygen and weaker signals from other atoms. The outcome was comparable with (Caroling et al 2013).

AFM analysis of nanoparticles

S. boulardii generated ZnO NPs with an average diameter of 62.89 nm and an average roughness of 6.025 nm, according to atomic force microscope (AFM) examination (Figure) (5, 6).

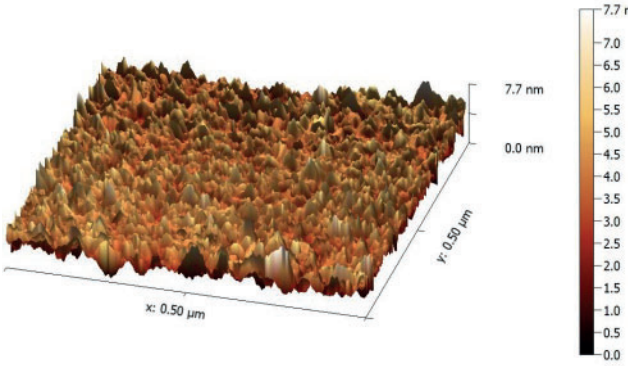

Figure (5) AFM analysis shows three-dimension image, and topography of biogenic ZnO NPs synthesis by *S. bularedii*

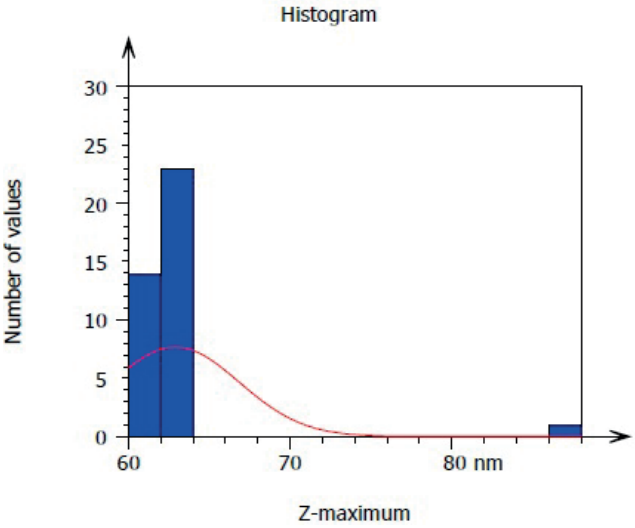

Figure (6) Granularity and accumulation distribution chart of biogenic ZnO NPs synthesis by *S. bularedii*

ZnO NPs' three-dimensional forms were revealed by AFM examination, and the average diameter of ZnO NPs derived from S. boulardii was 62.89 nm. This result may be attributed to differences in the bio-reduction that may be return to the qualitative and quantitative of extracellular protein/enzyme and other biomolecules that offered in the culture of each microorganism, in addition to their ability of interaction with precursor for synthesized (Zinc acetate). Nanoparticles amalgamation was better in terms of quality; minimum size and less polydispersity, with S. bularedii (Chaudhari, et al 2012).

Fourier Transform Infrared Spectroscopy (FTIR) analysis of nanoparticles

The FTIR spectrum displays distinct functional groups at various places; the wavenumber ranges from 400 cm-1 to 4000 cm-1, and the peak areas below and above 1500 cm-1 are referred to as the fingerprinting region and diagnostic region, respectively (Onyszko

et al 2022). Figure 7 shows the diagnostic area for the ZnO NPs produced by S. bularedii, which includes broad band peaks at 3448 cm-1 for O-H stretching, 2923 cm-1 for C-H stretching vibration of alkane groups, 2343 cm-1 for C-C stretching, and 1637 cm-1 for C-C stretching (alkene). These findings are consistent with (Kaschner et al 2002)

Antibacterial activity

The results demonstrated that both gram positive and gram negative bacteria can grow more slowly when exposed to ZnO NPs. Gram negative bacteria had a larger inhibitory zone than gram positive bacteria. At a concentration of 200 g/ml, ZnO NPs produced by S. bularedii exhibited the maximum inhibition against P. mirabilis (22 2.8) and the lowest impact against P. aeruginosa (17 3.1). These results are in accordance with (Dobrucka & Dugaszewska 2016). The investigation also revealed (P 0.05), Table significant differences between the various concentrations (3).

ZnO nanoparticles, according to (Divya et al 2013), damage bacterial membranes most likely by producing reactive oxygen species including superoxide and hydroxyl radicals. This is dependent on the type of surface that certain bacteria have. Additionally, according to reports, the antibacterial activity is influenced by the kind of surfactant utilized as well as the ZnO nanoparticle concentration. Additionally, ZnO nanoparticles may have caused bacterial cell membrane disruption and expulsion of cytoplasmic contents, which led to the death of the bacteria (Divyapriya et al 2014).

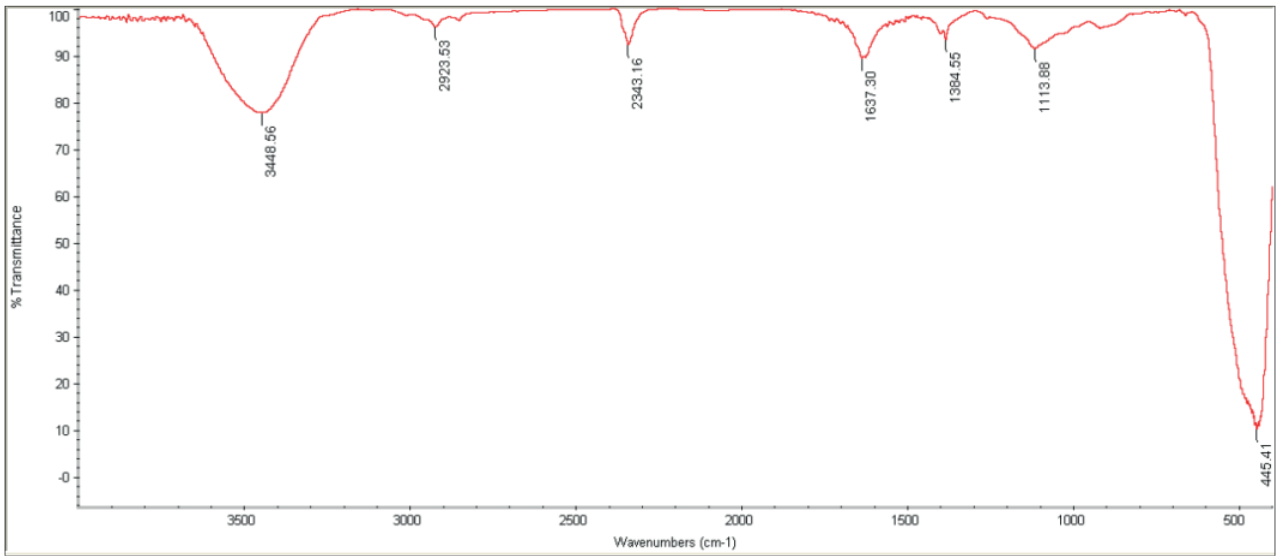

Figure (7): Fourier-transform infrared spectroscopy (FTIR) spectra of ZnO NPs synthesized by S. bularedii

Table (3)

Antibacterial activity of the ZnO NPs synthesis by S. bularedii against the tested bacteria as demonstrated by diameters of the inhibition zone (mm).

(A)	(D)	(B) / (C)(µg/ml)	Inhibition zone (mm) (Mean±S.D)		
			S. bularedii		
			50	100	200
ZnO NPs	S. aureus		16±1.1	16±1.9	20±0.4
	E. coli		17±0.6	18±1.8	20±0.2
	P. aeruginosa		12±0.8	16±0.2	17±3.1
	K. pneumonia		17±0.3	18±0.7	20±3.0
	P.mirabilis		15±0.7	18±1.1	22±2.8

$LSD_{(0.05)(A*B*C*D)}$ =1.992
A: type of nanoparticles
B: S. bularedii used for synthesized nanoparticles
C: Concentration of nanoparticles
D: pathogenic bacteria

Antibiofilm activity of zinc oxide nanoparticles

The quantitative measurement of biofilm production is done using the microtiter plate technique (Peerzada et al 2022). We selected one isolate from Gram positive bacteria and one from Gram negative bacteria from earlier study since all of the isolates produced biofilm. Different doses of biogenic ZnO NPs were investigated for anti-biofilm action against two bacterial strains, including (S. aureus and P. mirabilis). Based on earlier studies (Panda et al. 2016; Sultan & Nabiel, 2019), biofilm formation was computed and classified as strong, moderate, or non/weak. In this study, the development of biofilms decreased as ZnO NP concentration increased; the strongest inhibition was at a concentration of (1024 g/ml), and the lowest inhibition was at a concentration of (4 g/ml), Table (4, 5).

Additionally, the study demonstrated that there were variations in biofilm formation caused by S. bularedii-produced nanoparticle concentration and their impact on S. aureus and P. mirabilis at a significant level of (P 0.05), as shown in the table (6).

Table (4)
Effect of ZnO NPs from *S.bularedii* on S. *aureus* biofilm

non/weak	OD	inhibition%	moderate	OD	inhibition%	stronge	OD	inhibition%	control	OD
1024 µg/ml	0.007	97.19	**64 µg/ml**	0.122	50.22	**2 µg/ml**	0.245	0.00	**control**	0.245
512 µg/ml	0.009	96.25	**32 µg/ml**	0.126	48.59					
256 µg/ml	0.012	95.07	**16 µg/ml**	0.159	35.30					
128 µg/ml	0.118	51.73	**8 µg/ml**	0.187	23.97					
			4 µg/ml	0.232	5.30					

Table (5)
Effect of ZnO NPs from *S.bularedii* on *P.mirabilis* biofilm

non/weak	OD	inhibition%	moderate	OD	inhibition%	stronge	OD	inhibition%	control	OD
1024 µg/ml	0.006	97.70	**64 µg/ml**	0.128	52.71	**2 µg/ml**	0.270	0.00	**control**	0.270
512 µg/ml	0.012	95.44	**32 µg/ml**	0.175	35.32					
256 µg/ml	0.024	91.07	**16 µg/ml**	0.187	30.87					
128 µg/ml	0.092	65.79	**8 µg/ml**	0.23	13.90					
			4 µg/ml	0.233	13.57					

Table (6)
Prevention of multiple drug resistant bacterial biofilm formation by action of ZnO NPs synthesis by *S. bularedii*.

(A)	(B)	Inhibition biofilm formation (%) Mean±S.D	
		S. bularedii	
	(D) / (C) (µg/ml)	S. aureus	P. mirabilis
ZnO NPs	Control	0.00±0.0	0.00±0.0
	2	0.00±0.0	0.00±0.0
	4	5.30±0.3	13.60±1.2
	8	24.00±1.6	13.90±1.3
	16	35.30±2.2	30.90±1.1
	32	48.60±2.8	35.30±2.1
	64	50.20±3.1	52.70±2.2
	128	51.70±4.5	65.80±2.4
	256	95.10±2.9	91.10±2.9
	512	96.20±2.8	95.40±3.4
	1024	97.20±2.1	97.70±3.1

$LSD_{(0.05)(A*B*C*D)}$ = 0.909
A: type of nanoparticles
B: S. bularedii used for synthesized nanoparticles
C: Concentration of nanoparticles
D: pathogenic bacteria

Nanoparticles have the potential to change the expression of genes related to biofilm formation, which has an impact on the development of microcolonies and biofilms. The usage of these nanoparticles to create biofilm-related illnesses might be prevented and treated (González et al. 2015; Schmidt et al. 2017; Hassan, 2018).

Antioxidant activity of biogenic ZnO NPs

The capacity of nanoparticles to scavenge DPPH free radicals was demonstrated in the study by examining the transformation of DPPH from its original (purple) hue to its current (yellow) color. With higher concentrations, ZnO NPs become more efficient at scavenging DPPH free radicals. The lowest inhibition was at a dosage of 0.12 mg/ml, whereas the maximum inhibition was at 1 mg/ml. Additionally, the study found that there were substantial variations in the amounts of ZnO NPs produced by S. bularedii (p 0.05). According to the table (7).

Table (7)
Antioxidant activity of nanoparticles synthesized by *S. bularedii*, and influence of different concentration.

(A)	(B) / (C) mg /ml	Scavenging percentage (%) Mean±S.D
		S. bularedii
ZnO NPs	Control	0.00±0.00
	1	73.79±6.11
	0.5	73.04±4.32
	0.25	71.22±3.99
	0.12	69.58±2.06

$LSD_{(0.05)(A*B*C)}$ =0.429
A: type of nanoparticles
B: *S. bularedii* used for synthesized nanoparticles
C: Concentration of nanoparticles

The level of inhibition changes from one type of nanoparticle to another owing to an electron donation and DPPH acceptance (Kanipandian et al 2014; Bhakya et al 2015).

References

1. Abdulhassan, A. J. (2016). Effect of Silver and Titanium Nanoparticles Synthesized by Lactobacillus as Antimicrobial, Antioxidant and Some Physiological Parameters (Doctoral dissertation, Master Thesis. University of Kufa, Faculty of Science–Iraq).
2. Bahrulolum, H., Nooraei, S., Javanshir, N., Tarrahimofrad, H., Mirbagheri, V. S., Easton, A. J., & Ahmadian, G. (2021). Green synthesis of metal nanoparticles using microorganisms and their application in the agrifood sector. Journal of Nanobiotechnology, 19(1), 1-26.
3. Barapatre, A., Aadil, K. R., & Jha, H. (2016). Synergistic antibacterial and antibiofilm activity of silver nanoparticles biosynthesized by lignin-degrading fungus. Bioresources and Bioprocessing, 3(1), 1-13.
4. Begum, S. J., Pratibha, S., Rawat, J. M., Venugopal, D., Sahu, P., Gowda, A., ... & Jaremko, M. (2022). Recent Advances in Green Synthesis, Characterization, and Applications of Bioactive Metallic Nanoparticles. Pharmaceuticals, 15(4), 455.
5. Bhakya, S.; Muthukrishnan, S.; Sukumaran, M. and Muthukumar, M.(2015). Biogenic synthesis of iron nanoparticles and their antioxidant and antibacterial activity. Appl Nanosci., 6 (5):755–766.
6. Caroling, G.; Tiwari, S.K.; Ranjitham, A.M. and Suja, R .(2013). Biosynthesis of Zinc nanoparticles using aqueous broccoli extract-characterization and study of antimicrobial, cytotoxic effects . Asian J Pharm Clin Res., 6 (4): 165-172.
7. Chaudhari, P. R., Masurkar, S. A., Shidore, V. B., & Kamble, S. P. (2012). Antimicrobial activity of extracellularly synthesized silver nanoparticles using Lactobacillus species obtained from VIZYLAC capsule. Journal of Applied Pharmaceutical Science, (Issue), 25-29.
8. Dahiya, D., & Nigam, P. S. (2022). The Gut Microbiota Influenced by the Intake of Probiotics and Functional Foods with Prebiotics Can Sustain Wellness and Alleviate Certain Ailments like Gut-Inflammation and Colon-Cancer. Microorganisms, 10(3), 665.
9. Divya, M. J., Sowmia, C., Joona, K., & Dhanya, K. P. (2013). Synthesis of zinc oxide nanoparticle from Hibiscus rosa-sinensis leaf extract and investigation of its antimicrobial activity. Res. J. Pharm. Biol. Chem, 4(2), 1137-1142.
10. Divyapriya, S., Sowmia, C., & Sasikala, S. (2014). Synthesis of zinc oxide nanoparticles and antimicrobial activity of Murraya Koenigii. World J. Pharm. Pharm. Sci, 3(12), 1635-1645.
11. Dobrucka, R., & Długaszewska, J. (2016). Biosynthesis and antibacterial activity of ZnO nanoparticles using Trifolium pratense flower extract. Saudi journal of biological sciences, 23(4), 517-523.
12. Dobrucka, R., & Długaszewska, J. (2016). Biosynthesis and antibacterial activity of ZnO nanoparticles using Trifolium pratense flower extract. Saudi journal of biological sciences, 23(4), 517-523.

13. Durán, N., Marcato, P. D., Durán, M., Yadav, A., Gade, A., & Rai, M. (2011). Mechanistic aspects in the biogenic synthesis of extracellular metal nanoparticles by peptides, bacteria, fungi, and plants. Applied microbiology and biotechnology, 90(5), 1609-1624.
14. González, A.G.; Mombo, S.; Leflaive, J.; Lamy, A.; Pokrovsky, O.S. and Rols, J.L. (2015). Silver nanoparticles impact phototrophic biofilm communities to a considerably higher degree than ionic silver. Environ Sci Pollut Res Int. 22(11):8412-24.
15. Goyal, A. K., Middha, S. K., & Sen, A. (2010). Evaluation of the DPPHradical scavenging activity, total phenols and antioxidant activities in Indian wild Bambusa vulgaris" Vittata" methanolic leaf extract. Journal of Natural Pharmaceuticals, 1(1).
16. Hassan, H. H. (2018). Biosynthesis and characterization of Ag Nanoparticles from Klebsiella pneumoniae (Doctoral dissertation, University of Kufa).
17. Joerger, R., Klaus, T., & Granqvist, C. G. (2000). Biologically produced silver–carbon composite materials for optically functional thin-film coatings. Advanced Materials, 12(6), 407-409.
18. Kanipandian, N., Kannan, S., Ramesh, R., Subramanian, P., & Thirumurugan, R. (2014). Characterization, antioxidant and cytotoxicity evaluation of green synthesized silver nanoparticles using Cleistanthus collinus extract as surface modifier. Materials Research Bulletin, 49, 494-502.
19. Kaschner, A., Haboeck, U., Strassburg, M., Strassburg, M., Kaczmarczyk, G., Hoffmann, A., ... & Meyer, B. K. (2002). Nitrogen-related local vibrational modes in ZnO: N. Applied Physics Letters, 80(11), 1909-1911.
20. Loganathan, S., Shivakumar, M. S., Karthi, S., Nathan, S. S., & Selvam, K. (2021). Metal oxide nanoparticle synthesis (ZnO-NPs) of Knoxia sumatrensis (Retz.) DC. Aqueous leaf extract and It's evaluation of their antioxidant, anti-proliferative and larvicidal activities. Toxicology Reports, 8, 64-72.
21. Mohd Yusof, H., Rahman, A., Mohamad, R., Zaidan, U. H., & Samsudin, A. A. (2020). Biosynthesis of zinc oxide nanoparticles by cell-biomass and supernatant of Lactobacillus plantarum TA4 and its antibacterial and biocompatibility properties. Scientific reports, 10(1), 1-13.
22. Onyszko, M., Markowska-Szczupak, A., Rakoczy, R., Paszkiewicz, O., Janusz, J., Gorgon-Kuza, A., ... & Mijowska, E. (2022). The cellulose fibers functionalized with star-like zinc oxide nanoparticles with boosted antibacterial performance for hygienic products. Scientific Reports, 12(1), 1-13.
23. Ovais, M., Khalil, A. T., Ayaz, M., Ahmad, I., Nethi, S. K., & Mukherjee, S. (2018). Biosynthesis of metal nanoparticles via microbial enzymes: a mechanistic approach. International journal of molecular sciences, 19(12), 4100.
24. Panda, P. S., Chaudhary, U., & Dube, S. K. (2016). Comparison of four different methods for detection of biofilm formation by uropathogens. Indian Journal of Pathology and Microbiology, 59(2), 177.
25. Peerzada, Z., Kanhed, A. M., & Desai, K. B. (2022). Effects of active compounds from Cassia fistula on quorum sensing mediated virulence and biofilm formation in Pseudomonas aeruginosa. RSC Advances, 12(24), 15196-15214.
26. Rajeshkumar, S., & Malarkodi, C. (2014). In vitro antibacterial activity and mechanism of silver nanoparticles against foodborne pathogens. Bioinorganic chemistry and applications, 2014.
27. Ramesh, P., Saravanan, K., Manogar, P., Johnson, J., Vinoth, E., & Mayakannan, M. (2021). Green synthesis and characterization of biocompatible zinc oxide nanoparticles and evaluation of its antibacterial potential. Sensing and Bio-Sensing Research, 31, 100399.
28. Ranganath, E., Rathod, V., & Banu, A. (2012). Screening of Lactobacillus spp, for mediating the biosynthesis of silver nanoparticles from silver nitrate. IOSR Journal of Pharmacy, 2(2), 237-241.
29. Schmidt, H.; Thom, M.; Madzgalla, M.; Gerbersdorf, S.U.; Metreveli, Gand Manz, W. (2017). Exposure to Silver Nanoparticles Affects Biofilm Structure and Adhesiveness. J Aquat Pollut Toxicol. 1(2):9.
30. Shafaghat, A. (2015). Synthesis and characterization of silver nanoparticles by phytosynthesis method and their biological activity. Synthesis and Reactivity in Inorganic, Metal-Organic, and Nano-Metal Chemistry, 45(3), 381-387.
31. Shirley, B., & Jarochowska, E. (2022). Chemical characterisation is rough: the impact of topography and measurement parameters on energy-dispersive X-ray spectroscopy in biominerals. Facies, 68(2), 1-15.
32. Singh, N., Armstrong, D.G., and Lipsky, B.A. (2005). Preventing foot ulcers in patients with diabetes. J.Am.Med.Ass. 293,217–228.doi: 10.1001/jama.293.2.217
33. Sultan, A. M., & Nabiel, Y. (2019). Tube method and Congo red agar versus tissue culture plate method for detection of biofilm production by uropathogens

isolated from midstream urine: Which one could be better?. African Journal of Clinical and Experimental Microbiology, 20(1), 60-66.
34. Veve, M. P., Mercuro, N. J., Sangiovanni, R. J., Santarossa, M., & Patel, N. (2022, June). Prevalence and Predictors of Pseudomonas aeruginosa among Hospitalized Patients with Diabetic Foot Infections. In Open Forum Infectious Diseases.
35. Yallappa, S., Manjanna, J., Sindhe, M. A., Satyanarayan, N. D., Pramod, S. N., & Nagaraja, K. (2013). Microwave assisted rapid synthesis and biological evaluation of stable copper nanoparticles using T. arjuna bark extract. Spectrochimica Acta Part A: Molecular and Biomolecular Spectroscopy, 110, 108-115.
36. Zhang, S., Lin, L., Huang, X., Lu, Y. G., Zheng, D.L., & Feng, Y. (2022). Antimicrobial Properties of Metal Nanoparticles and Their Oxide Materials and Their Applications in Oral Biology. Journal of Nanomaterials, 2022.